Pressure Drop in Horizontal Two-Phase Flow

Safa Subhi Ibrahim
Petroleum Engineering Department
University of Zakho
Zakho City, Kurdistan Region-Iraq
Safa.ibrahim@uoz.edu.krd

Lokman Aziz Abdulkareem
Petroleum Engineering Department
University of Zakho
Zakho City, Kurdistan Region-Iraq
lokman.abdulkareem@uoz.edu.krd

Received: 25 June 2022 | Revised: 12 July 2022 | Accepted: 12 July 2022

Abstract-In an artificial environment, the most important key in the process equipment design is determining gas-liquid two-phase flow frictional pressure drop of pipes. To achieve this, an experimental investigation was carried out in this study to analyze the pressure drops of air-water two-phase flow in a 30mm internal diameter horizontal pipe with a length of 6m at different flow conditions. The study was carried out at 20C^0 using tap water and air. To cover the slug flow pattern, the volumetric flow rate of water varied from 30 to 80 LPM, and the volumetric flow rate of air from 40 to 200 LPM. Pressure transmitters were used to measure pressure at four different points along the test section, each 2m apart. The results of the experiments were compared to 8 models using 3 distinct methods: Mean Absolute Percentage Error (MAPE), Relative Performance Factor (RPF), and the percentage of data included in the range of the 30% error band. All methods produced similar results, with the Sun-Mishima model being the most accurate.

Keywords-two-phase flow; frictional pressure drop; slug experimental model; horizontal flow; homogenous and separated flow model

I. INTRODUCTION

Many industrial applications, such as heat exchangers, pipeline network systems, refrigeration and heat pumps, thermal energy plants, environmental control, life-support systems, and fuel cells rely on the measurement of pressure drop in two phases [1, 2]. Furthermore, the pressure drop is essential because the co-current flow of liquid and gas causes design and operational problems due to the formation of various types of two-phase flow patterns. In these cases, estimating pressure drop helps the piping designer in determining the optimal line size and designing a better piping system [3-5].

During the past 60 years, investigators have been researching two-phase frictional pressure drop. A comprehensive theoretical and experimental research was carried out and various relationships were proposed in [6]. For estimating the frictional pressure drop in horizontal and vertical pipes, there are two types of models: homogeneous and separated flow models. In homogeneous flow, the two phases are considered to be intimately mixed with no relative motion between them, either locally or overall [6]. Thome suggested utilizing the homogeneous model for mass fluxes more than 2000kg/m^{2}s at high-reduced pressures and higher mass velocities [7]. The separated flow, on the other hand, recognizes that the two phases can exist separately, each flowing through its own pipe, with the assumption that the velocity of each phase is constant in the zone occupied by the phase [8-14].

Some researchers assessed a few correlations using limited experimental data. Authors in [15] used R134a, R123, R402A, R404A, and R502 evaporation data in two horizontal pipes with 10.92 and 12.0mm ID (Inner Diameter), with mass flux ranging from 100 to 500kg/m^{2}s and vapor quality ranging from 0.04 to 1.0, to evaluate 7 models. Overall, authors in [16, 17] proposed the most accurate predictors, with the one in [10] being the third-best prediction. Authors in [18] validated 15 equations based on experimental data of R410A convective boiling in two pipes of 1.5 and 3mm ID, with inlet saturation temperature of 10^{o}C, mass flux of 300 to 600kg/m^{2}s, and heat flux of 10 to 40kW/m^2. They discovered that a homogeneous approach could accurately predict frictional pressure drop. Authors in [19] compared 11 correlations to empirical observations of R123, R134a, R22, R236ea, R245fa, R404A, R407C, R410A, R507, CO_2, water, and air, with hydraulic diameters ranging from 0.506 to 12mm, Re_l ranging from 10 to 37,000, and Re_g ranging from 3×10^5 to 4×10^5. The results showed that the correlations in [8, 12, 20, 21] performed similarly in the viscous region, while the Muller-Steinhagen and Heck [17] correlation performed best in the turbulent region. Authors in [21] tested 10 correlations against a variety of experimental data sets using a separated flow approach. According to the results, the correlations of [21] had the highest accuracy. Authors in [22, 23] studied the possibility of calculating two-phase frictional pressure drop in microgravity using normal gravity two-phase frictional pressure drop correlations. Microgravity experimental data were compared to 23 two-phase frictional pressure drop correlations. The above evaluations based on normal gravity experimental data produced inconsistencies. The homogeneous model [18, 24, 21], the Chen et al. correlation [23], and the Zhang et al. formula [21] have been proposed, whereas authors in [15, 19, 25] suggested the Muller-Steinhagen and Heck [17] correlation as the best prediction. The effects of fluid refrigerant and channel geometry on the frictional pressure drop during two-phase flow of R134a, R1234ze(E), R1234yf and R600a in a horizontal tube with mass velocities varying between 100 and 1600kg/m^{2}s, saturation temperatures of 31 and 41°C and vapor

Corresponding author: Safa Subhi Ibrahim

quality from 0.05 to 0.95 was investigated in [26]. They concluded that the new method accurately predicted the database, predicting 89% of the results within an error band ±20%. Authors in [27] studied experimentally the pressure drop of evaporative propane with mass flux of 360 to 915kg/m^{2}s and vapor quality of 0 to 1.0 in microchannel with 500μm diameter and 0.5m length. Authors in [28] conducted an experimental analysis of the frictional pressure drop in a plate heat exchanger using the working fluid R-1233zd(E). According to the experimental findings, the frictional pressure drop increases with increasing mass flux and mean vapor quality while it decreases with increasing saturation pressure. The experimental results led to the development of correlations for the friction factor of R1233zd(E) in plate heat exchangers. The new correlation of the friction pressure drop and mixture viscosity for two phase flow in homogenous approach modeling was developed in [1] and was compared to 846 experimental data of friction pressure drop that were collected from previous studies. The experimental data including various working fluids such as R1234ze(E), R32, R-600a R717, R134a, R410A and carbon dioxide (CO_2) at various hydraulic IDs and mass flux. The discovered Mean Absolute Relative Deviation (MARD) was 30%. These new correlations of two-phase flow pressure drop were used to predict the experiment measurements of pressure drop on circular pipes, mini-channels, and micro-channels. The experimental data used for their evaluations were rare, which could be the root cause of the inconsistency. Furthermore, the number of correlations examined in each paper was limited to no more than 15 in total. A complete evaluation is therefore necessary. This article has conducted a review of the literature on two-phase frictional pressure drop correlations for homogeneous and separated flows for finding an optimal model for experimental data.

II. PRESSURE DROP IN HORIZONTAL TWO-PHASE FLOW

Two-phase pressure drop predicting methods in horizontal pipes are discussed in this article. The sum of the static pressure drop (elevation head) ΔP_{static}, momentum pressure drop (acceleration) ΔP_{acce}, and frictional pressure drop ΔP_{frict} is the total measured pressure drop ΔP_{total} of a fluid in a horizontal two-phase flow pipe [7]:

$$\Delta P_{total} = \Delta P_{static} + \Delta P_{acce} + \Delta P_{frict} \quad (1)$$

The gravitational pressure drop ΔP_{static} in a horizontal pipe is zero, and the quality is constant throughout the pipe (as a result, in adiabatic flow, the acceleration term appears to have no effect on the pressure drop and can be ignored). Only the frictional pressure drop was studied. The following two classic models are used for two-phase flows.

A. Homogeneous Flow Model

Because gas and liquid have similar velocities in the homogeneous flow model, the frictional pressure drop for two-phase flow can be rewritten as [29]:

$$(\frac{dp}{dz})_{Tp,hom} = (\frac{2f_{Tp}G_{Tp}^2}{D\rho_{Tp}})_{Tp,hom} \quad (2)$$

where f_{Tp} is the friction factor for smooth pipe based on Petukhov correlation (where: $f_{Tp} = (0.79\ \ln Re_{Tp} - 1.64)^{-2}$) [23], G_{Tp} is the two-phase mass flux (kg/m^{2}s), D is the diameter of the pipe (m), ρ_{Tp} is the two-phase flow density (kg/m^3), and Re_{Tp} is the two-phase flow Reynolds number. The values of ρ_{Tp} and Re_{Tp} are calculated as [1]:

$$\rho_{Tp} = (\frac{x}{\rho_g} + \frac{1-x}{\rho_l})^{-1} \quad (3)$$

$$Re_{Tp} = \frac{G_{Tp}D}{\mu_{Tp}} \quad (4)$$

where:

$$\mu_{Tp} = (\frac{x}{\mu_g} + \frac{1-x}{\mu_l})^{-1} \quad (5)$$

where μ_{Tp}, μ_l, and μ_g are the dynamic viscosities of two-phase, liquid, and gas (kg/ms) respectively [30], x is the air mass quality, and ρ_g and ρ_l are the densities of gas and liquid phases (kg/m^3) respectively. According to the homogeneous flow, the correlations of frictional pressure drop are: McAdams [30] and Chen et al [13]. Table I contains more information.

TABLE I. HOMOGENEOUS CORRELATIONS

Reference	Correlations
[30]	(2)
[13]	$(\frac{dp}{dz})_{Tp} = \Omega_{ch}(\frac{dp}{dz})_{Tp,hom}$ where Ω_{ch} parameter depends on Bond number Bo: $\Omega_{ch} = \begin{cases} 1.2 - 0.9\exp(-Bo) & Bo < 2.5 \\ 1 + \frac{We_{Tp}^{0.2}}{\exp(Bo^{0.3})} - 0.9\exp(-Bo) & Bo \geq 2.5 \end{cases}$ in which, $Bo = \frac{g(\rho_l - \rho_g)(D/2)^2}{\sigma}$ and $We_{Tp} = \frac{G_{Tp}^2 D}{\sigma\rho_{Tp}}$ where g is the gravity acceleration (m/s^2), We_{Tp} is the two-phase Weber No. (-), and σ is the surface tension of water (N/m).

B. Separated Flow Model

This model is based on the use of the two-phase friction multiplier φ_i^2, where the subscript i can be l, g, l_o, or g_o indicating liquid, gas, liquid-only, or gas-only respectively. The separated flow is divided into two branches:

1) Liquid and Gas Frictional Multipliers ($\emptyset_l^2$ and $\emptyset_g^2$)

Two-phase friction multiplier method depends on liquid (φ_l^2) and gas (φ_g^2). The frictional multiplier is the ratio of the two-phase frictional pressure drop to the single-phase frictional pressure drop as follows [9]:

$$\varphi_i^2 = (\frac{dp}{dz})_{Tp} / (\frac{dp}{dz})_i \quad (6)$$

where:

$$\left(\frac{dp}{dz}\right)_i = \frac{2f_i G_i^2}{D\rho_i} \quad (7)$$

where the subscript i can be l or g denoting liquid or gas respectively, $(\frac{dp}{dz})_i$ is the single-phase frictional pressure drop (KPa/m), f_i is the friction factor, and G_i is the actual mass flux (kg/m^{2}s). Based on [23], the friction factor of liquid and gas for a smooth pipe can be calculated as:

$$f_i = 0.25\left[log\left(\frac{150.39}{Re_i^{0.98865}} - \frac{152.66}{Re_i}\right)\right]^{-2} \quad (8)$$

and the Re_ivalues for each phase can be calculated as [1]:

$$Re_i = \frac{G_i D}{\mu_i} \quad (9)$$

Authors in [8] discovered that ϕ_l^2 and ϕ_g^2 are functions of the dimensionless variable X in the following way [8]:

$$X = \sqrt{\frac{(dp/dz)_l}{(dp/dz)_g}} \quad (10)$$

where X is the Lockhart-Martinelli parameter. Many other researchers' studies and correlations were inspired by this model. According to the separated flow model, the frictional pressure drop correlations are: Chisholm [31], and Sun-Mishima [19]. Table II contains additional information.

TABLE II. THE SEPARATED CORRELATIONS: LIQUID AND GAS FRICTIONAL MULTIPLIERS (ϕ_l^2 AND ϕ_g^2).

Reference	Correlations
[31]	$\boldsymbol{\phi_l^2 = 1 + \frac{C}{X} + \frac{1}{X^2}}$ C: 20 — Gas: Turbulent — Liquid: Turbulent C: 12 — Gas: Turbulent — Liquid: Laminar C: 10 — Gas: Laminar — Liquid: Turbulent C: 5 — Gas: Laminar — Liquid: Laminar
[19]	For viscous flow: $\boldsymbol{C = 26\left(1 + \frac{Re_l}{1000}\right)[1 - \exp\left(\frac{-0.153}{0.8 + 0.27La}\right)]}$ where La is the Laplace number, for turbulent flow: $\phi_l^2 = 1 + \frac{C}{X^{1.19}} + \frac{1}{X^2}$, where: $C = 1.79\left(\frac{Re_g}{Re_l}\right)^{0.4}\sqrt{\frac{1-X}{X}}$, $Re_g = G_{Tp}xD/\mu_g, and\ Re_l = G_{Tp}(1-x)D/\mu_l$

2) Liquid-Only and Gas-Only Frictional Multipliers (φ_{lo}^2 and φ_{go}^2)

The frictional multipliers in this case are defined as the ratio of the two-phase frictional pressure gradient over the pressure gradient that would arise if the phase flowed alone in the pipe to the total mass flux of the two-phase flow [31]:

$$\varphi_i^2 = (\frac{dp}{dz})_{Tp} / (\frac{dp}{dz})_i \quad (11)$$

where the subscript i can be l_o, or g_o indicating liquid-only, or gas-only respectively. The single-phase frictional pressure drop is computed as follows:

$$(\frac{dp}{dz})_i = \frac{2f_i G_{Tp}^2}{D\rho_i} \quad (12)$$

In this case, the Fang et al. correlation (8) was used to calculate the friction factor. Table III displays the frictional pressure drop correlations for this method.

TABLE III. THE SEPARATED CORRELATIONS: LIQUID-ONLY AND GAS- ONLY FRICTIONAL MULTIPLIERS (Φ_{LO}^2 AND Φ_{GO}^2).

Reference	Correlations
[9]	$\phi_{lo}^2 = 1 + (Y^2 - 1)\{B[(1-x)]^{0.875} + x^{1.75}$ where: $Y^2 = (\frac{dp}{dz})_{go} / (\frac{dp}{dz})_{lo}$ $If\ 0 < Y < 9.5, B = \begin{cases} 55/G_{Tp}^{0.5} & G_{Tp} \geq 1900 \\ 2400 & 500 < G_{Tp} < 1900 \\ 4.8 & G_{Tp} \leq 500 \end{cases}$ $If\ 9.5 < Y < 28, B = \begin{cases} 520/YG_{Tp}^{0.5} & G_{Tp} \leq 600 \\ 21/Y & G_{Tp} > 600 \end{cases}$ $If\ Y > 28, B = 15000/Y^2 G_{Tp}^{0.5}$
[10]	For viscous flow: $\phi_{lo}^2 = (1-x)^2 + x^2\left(\frac{\rho_l f_{go}}{\rho_g f_{lo}}\right) + \frac{3.24x^{0.78}(1-x)^{0.224}H}{F_{Tp}^{0.45} We_{Tp}^{0.035}}$ where: $H = \left(\frac{\rho_l}{\rho_g}\right)^{0.91}\left(\frac{\mu_g}{\mu_l}\right)^{0.19}(1 - \mu\_g/\mu\_l)^{0.7}$, and, F_{Tp}=$G_{Tp}^2/gD\rho_{Tp}^2$
[16]	$\phi_{lo}^2 = 1 + (\frac{dp}{dz})_{Fr}[\left(\frac{\rho_l}{\rho_g}\right)\left(\frac{\mu_g}{\mu_l}\right)^{0.25} - 1]$ Where: $(\frac{dp}{dz})_{Fr} = f_{Fr}[x + 4(x^{1.8} - x^{10} f_{Fr}^{0.5})]$, $f_{Fr} = \begin{cases} 1 & Fr_{lo} \geq 1 \\ F_{lo}^{0.3} + 0.0055[\ln(\frac{1}{Fr_{lo}})]^2 & Fr_{lo} < 1' \end{cases}$ and $Fr_{lo} = G_{Tp}^2/gD\rho^2$
[17]	$\phi_{lo}^2 = Y^2x^3 + (1-x)^{1/3}[1 + 2x(Y^2 - 1)]$

III. EXPERIMENTAL SETUP AND MEASUREMENTS

The specially designed system was constructed to measure pressure drop in two-phase slug flow in a horizontal pipe. The two-phase air-water system was designed and built-up in the Multi-phase Laboratory of the Petroleum Engineering Department, College of Engineering, University of Zakho. The system's main components were the air and water supply systems, a two-phase mixer, a visual horizontal test section, pressure transmitters, and facility instrumentation. The air-water flow loop system scheme is illustrated in Figure 1.

The fluids in this system were air and water. A SHIMGE centrifugal water pump with a head of 22.5m and 600 LPM capacity was utilized to circulate water from a water storage tank to feed the test section via a water rotameter. The water rotameter was controlled by two ball valves and had a range of 20 to 150 LPM with an accuracy of ±4%. They were both used to control the amount of flow that entered the test section, passed through a horizontal pipe, and then to a separator/first tank. In the separator tank, the air was released into the atmosphere via the separator tank's top, and the liquid settled under gravity and flowed through the bottom to return to the second tank. The water was stored in the two tanks that were linked together with PVC pipe. The first tank housed the return water from the test section, while the second tank, with a capacity of 426L, was used to feed the system via a PVC pipe connected to the pump. The second tank's function was to keep air bubbles and debris from transferring from the tank to the pump and to control the pump's excess flow.

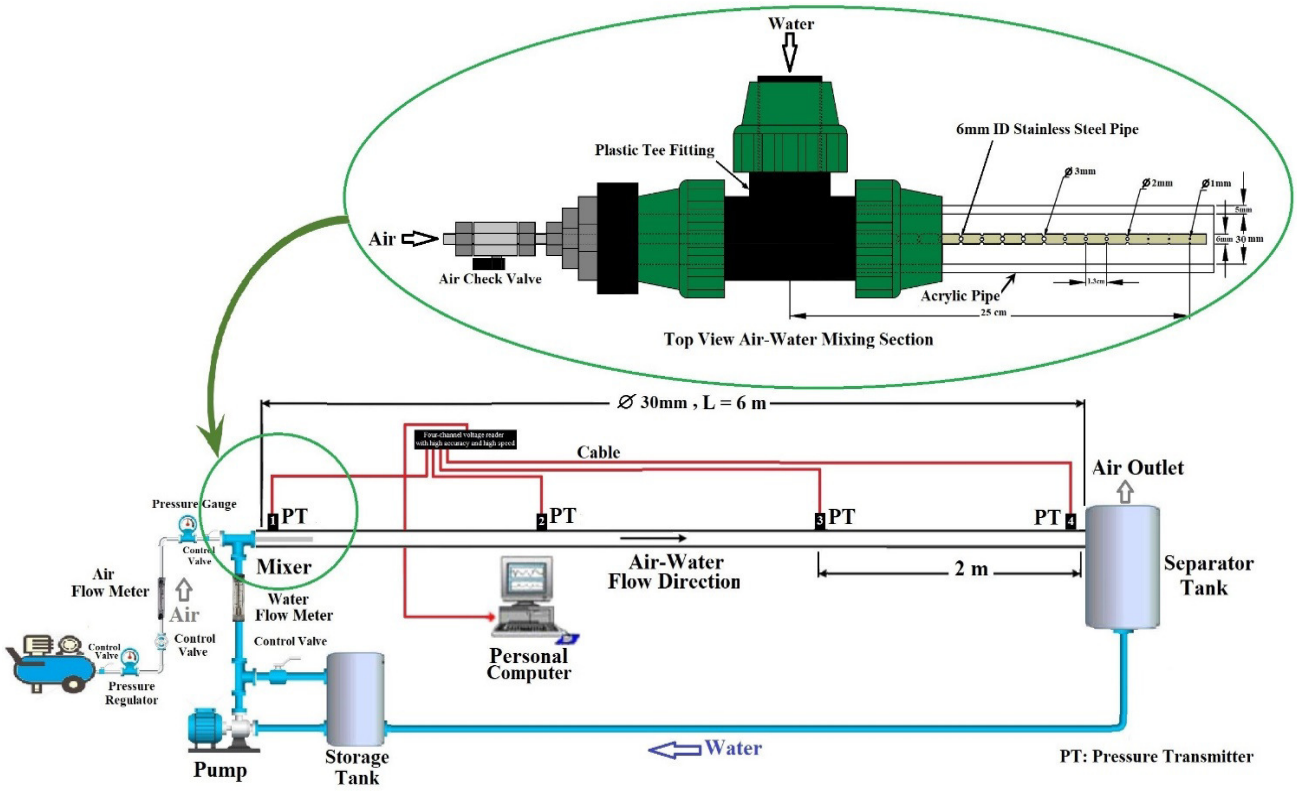

Fig. 1. The schematic diagram of the experimental facility.

Meanwhile, the compressor supplied air to the loop, which was controlled by an air filter regulator with 0-11 bar range. An air rotameter with a measuring range of 40 to 400LPM and accuracy of ±4% was utilized to measure the air flow rate. At the T-junction at the test section's entrance, air and water were mixed. Water from the pump was fed into the mixer from one side, while compressed air was charged into the mixer via a 6mm diameter flexible hose parallel to the main flow. To distribute the air in the water stream, a mixer was also used. The designs of [23, 33] were used in the mixing section. The mixer section was constructed of a 6mm stainless steel pipe and was installed in the water stream using a plastic T-junction and a compression fitting. The stainless-steel pipe was soldered to prevent air flow from the end. Sixty holes with 1.3cm spacing and varying diameters were drilled in 15 columns around the stainless-steel pipe over a length of 25cm (3 rows of 1mm, 4 rows of 2 mm, and 8 rows of 3 mm). To prevent water from entering the air flow, the size of the holes was decreased through the internal tube. The testing section was divided into 3 parts. Each part was constructed from the acrylic pipe with a visual thickness of 5mm, a length of 2m, and an ID of 30mm. Each of the 3 parts of the test section was connected using flange connections. The total length of the test section was 6m. The flanges were mounted on fixed rigid steel frames to ensure long-term support and safe operation. Moreover, 4 different pressure transmitters from the WIKI Company with a range of 0-2bar were fixed to the top of the test section pipe by brass pipe fittings and installed to measure the pressure difference along the test section. Figure 2 depicts the experimental setup. The strategy employed at the start of each run was to start with a fixed water discharge flow rate and gradually increase the air flow rate until slug flow appeared, then increase the water flow rate and repeat the previous steps. The Baker flow pattern map was used to determine experimental settings for the air-water flow rates [34]. These experimental conditions were scripted in Matlab (R2017b). The result is shown in Figure 3. The water and air flow rates were 30 to 80 LPM and 40 to 200 LPM respectively. The system's 4-channel voltage reader was utilized to read transient pressures from the pressure transmitter to a PC. The optimum time for all variable test requirements to exclude the influent effect on the flow was 30s. The experiments were conducted at a pressure of 1bar and a temperature of 20^{o}C. All the experimental operating conditions are displayed in Table IV.

Fig. 2. The experimental setup.

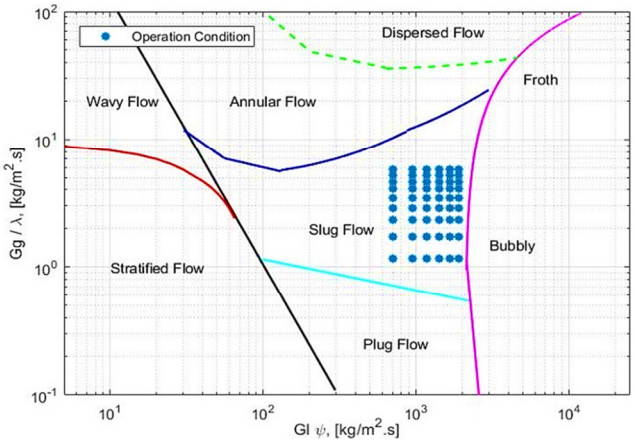

Fig. 3. Flow pattern map produced by Matlab (R2017b) based on the experimental operating conditions.

IV. RESULTS AND DISCUSSION

Statistical analysis was performed on the results of the two-phase pressure drop models to determine the best model among the 8 considered models. The results are shown in Table V. The analytic parameters are included in the following equations [35]:

$$e_i = \frac{\Delta P_{i\,cal} - \Delta P_{i\,exp}}{\Delta P_{i\,exp}} \quad (13)$$

$$E_1 = \frac{100}{n}\sum_{i=1}^{n} e_i \quad (14)$$

$$E_2 = \frac{100}{n}\sum_{i=1}^{n} |e_i| \quad (15)$$

$$E_3 = \sum_{i=1}^{n}\sqrt{\frac{(e_i - E_1)^2}{n-1}} \quad (16)$$

$$E_4 = \frac{1}{n}\sum_{i=1}^{n} e_i \quad (17)$$

$$E_5 = \frac{1}{n}\sum_{i=1}^{n} |e_i| \quad (18)$$

$$E_6 = \sum_{i=1}^{n}\sqrt{\frac{(e_i - E_4)^2}{n-1}} \quad (19)$$

E_1 is the Mean Percentage Error (MPE), E_2 is the Mean Absolute Percentage Error (MAPE), E_3 is the standard deviation percentage, E_4 is the mean error, E_5 is the mean absolute error, and E_6 is the standard deviation. According to Table V, the MAPE values for [13] and [30] were 18.54% and 29.15% respectively, for the homogeneous model, while for separated models, the model of [19] with 17.54% gives the least amount of MAPE, followed by the models of [17] with 28.53%, [9] with 28.99%, [10] with 35.14%, [16] with 41.70%, and [31] with 41.9%. It can be concluded that, out of the 8 models tested, the Sun-Mishima model [19] predicts the two-phase pressure drop with greater accuracy. The Relative Performance Factor (RPF) used to identify the best model is [36]:

$$\text{RPF} = \frac{|E_1|-|E_{1min}|}{|E_{1max}|-|E_{1min}|} + \frac{|E_2|-|E_{2min}|}{|E_{2max}|-|E_{2min}|} + \frac{|E_3|-|E_{3min}|}{|E_{3max}|-|E_{3min}|} + \frac{|E_4|-|E_{4min}|}{|E_{4max}|-|E_{4min}|} + \frac{|E_5|-|E_{5min}|}{|E_{5max}|-|E_{5min}|} + \frac{|E_6|-|E_{6min}|}{|E_{6max}|-|E_{6min}|} \quad (20)$$

For predicting two-phase pressure drop, the model with the least amount of RPF is the best, and the model with the most amount of RPF is the worst. In this method, [13] with 0.47 RPF value for homogeneous models and [19] with 0.76 RPF value for separated models produce the most accurate results, as displayed in Table V.

The third method investigates whether the data points fall within ±30% of the error band and the results are depicted in Table VI and Figures 4-9. The model of [13] results showed that most data points were within ±30% error band for homogeneous models. For the separated model, the models of [19] displayed the highest percentage of data with 88.9% of data within ±30% of the error band as illustrated in the Figures 4-9. These results differ from previous results, but the Sun-Mishima [19] model provides the best predictions of two-phase pressure drop models in each method.

TABLE IV. EXPERIMENTAL OPERATING CONDITIONS

Fluids	Temperature (C°)	Gas Flow Rate (LPM)	Water Flow rate (LPM)	Pressure (bar)	Data rerecording time	No. of Tests
Air-water	20°	40, 60, 80, 100, 120, 140, 160, 180, and 200	30, 40, 50, 60, 70, and 80	0-1	30s	54

TABLE V. ERROR RESULTS FOR EACH MODEL

Reference	MPE (E_1%)	MAPE (E_2%)	Standard Deviation Percentage (E_3)	Mean Error (E_4)	Mean Absolute Error (E_5)	Standard Deviation (E_6)	*RPF*
[30]	-25.99	29.15	190.83	-0.26	0.29	1.07	2.95
[13]	-5.73	18.54	42.05	-0.06	0.19	1.23	0.47
[31]	41.61	41.90	305.57	0.42	0.42	1.88	5.74
[19]	9.64	17.54	70.82	0.10	0.18	1.30	0.76
[9]	-21.73	28.99	159.60	-0.22	0.29	1.45	2.78
[10]	31.08	35.14	228.26	0.31	0.35	2.36	4.57
[16]	-41.21	41.70	302.64	-0.41	0.42	0.51	4.95
[17]	-23.40	28.53	171.85	-0.23	0.29	1.23	2.77
E-min	5.726	17.544	42.047	0.057	0.175	0.506	
E-max	41.612	41.895	305.571	0.416	0.419	2.362	

TABLE VI. DATA POINT PERCENTAGE WITHIN THE ±30% ERROR BAND

Model	[30]	[13]	[31]	[19]	[9]	[10]	[16]	[17]
±30%	50	88.9	55.6	88.9	51.9	68.5	0.0	59.3

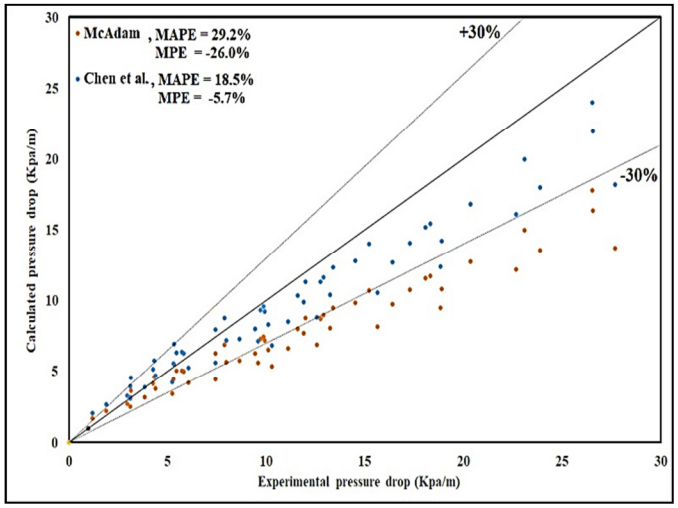

Fig. 4. Comparison of the experimental data with the McAdams [30] and Chen et. al [13] correlations.

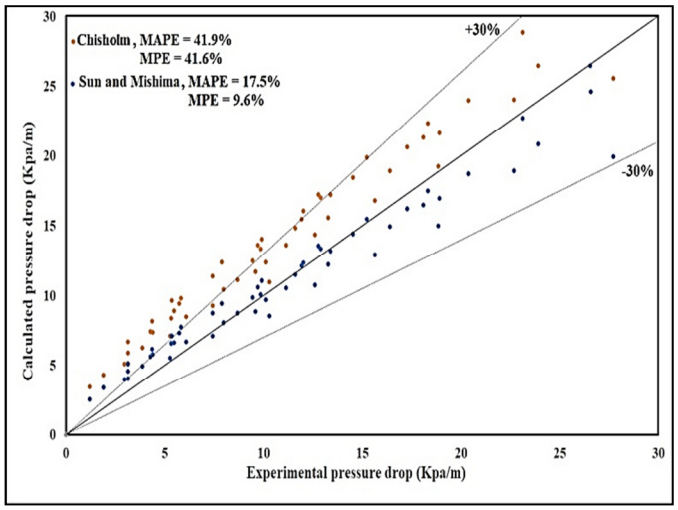

Fig. 5. Comparison of the experimental data with the Chisholm [31] and Sun-Mishima [19] correlations.

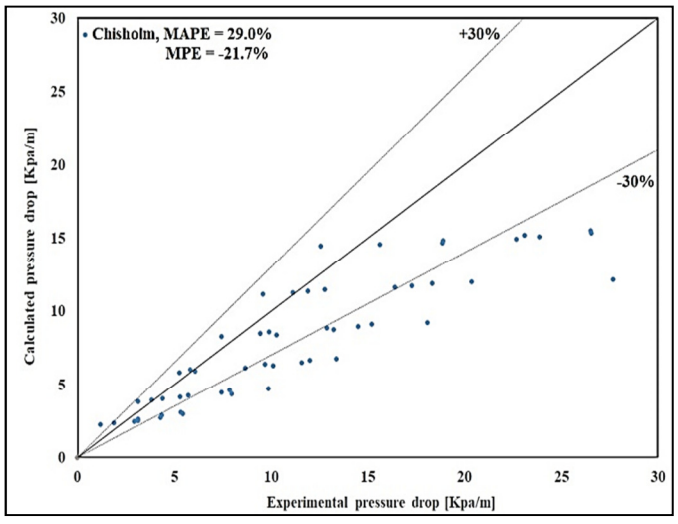

Fig. 6. Comparison of the experimental data with the Chisholm [9] correlation.

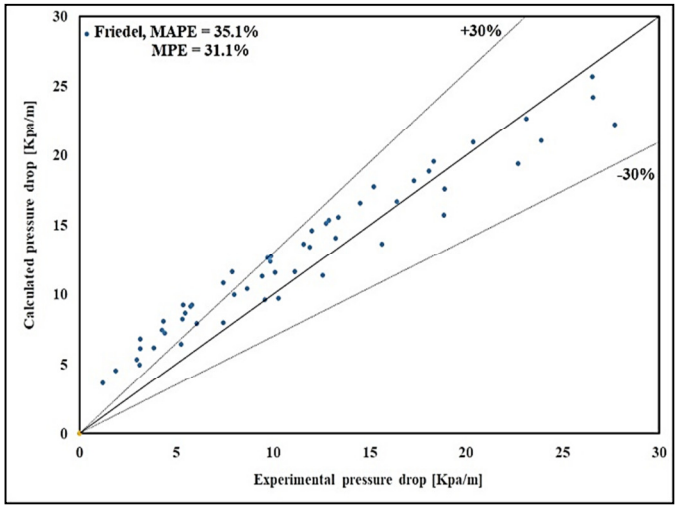

Fig. 7. Comparison of the experimental data with the Friedel correlation [10].

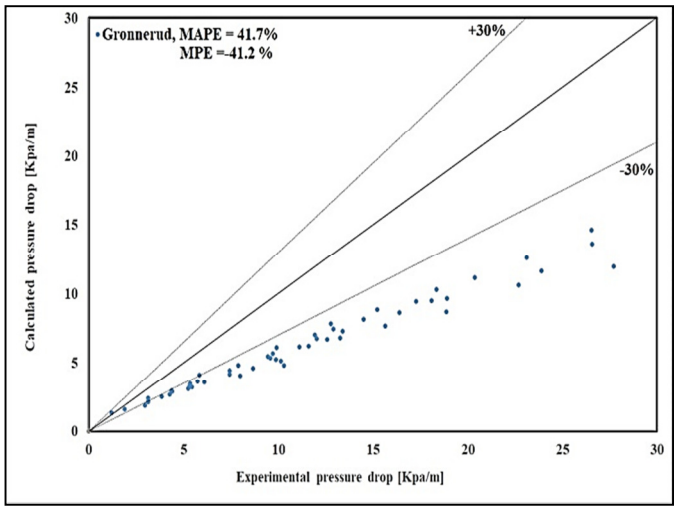

Fig. 8. Comparison of the experimental data with the Grounerud correlation [16].

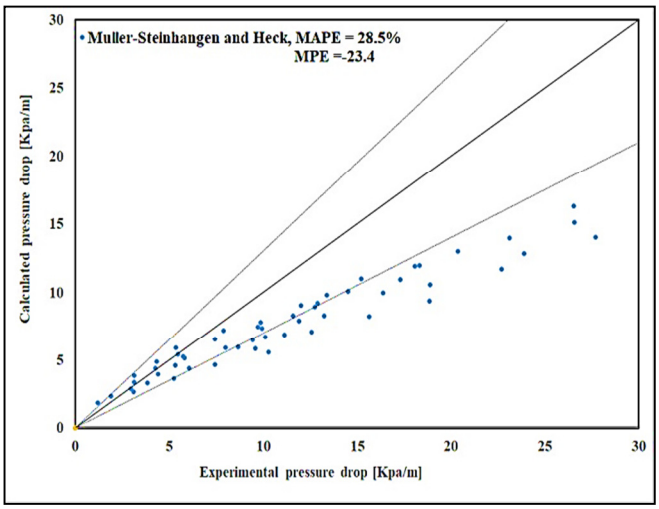

Fig. 9. Comparison of the experimental data with the Muller-Steinhangen and Heck correlation [17].

V. CONCLUSION

The current work evaluated 8 models based on experimental data of air-water flow that were chosen to rely on Baker map in a horizontal test section 6m long and with 30mm ID, and with discharge flow rates for water and air ranging from 30 to 80 LPM and 40 to 80 LPM respectively. Four pressure transmitters were used to measure the pressure along the test section, with a 30s ideal measurement period. The 54 experimental data points were compared to 8 well-known pressure drop models using a variety of methods. Some key findings of the current study are:

- MAPE was used to compare the experimental results to previous correlations. The Sun-Mishima model was found to be the best, with 17.54%, while the Müller-Steinhagen and Heck, Chisholm, Friedel, and Gronnerud models produce acceptable results. Chisholm is the least accurate model, with 41.9% accuracy.
- The results of the RPF comparison show that the outcomes were identical to the results of MAPE. The Sun-Mishima model had the highest RPF of 0.76, while the Chisholm model had the lowest.
- To evaluate these models, the percentage of data that falls within ±30% of the error band was used. The results of this method differ slightly from those of the previous methods, but ultimately, the Sun-Mishima model was again the most accurate, with 88.9% of data falling within the ±30% error band.

REFERENCES

[1] D. Maher, A. Hana, and S. Habib, "New Correlations for Two Phase Flow Pressure Drop in Homogeneous Flows Model," *Thermal Engineering*, vol. 67, no. 2, pp. 92–105, Feb. 2020, https://doi.org/10.1134/S0040601520020032.

[2] E. J. Suarez-Dominguez, E. F. Izquierdo-Kulich, A. Rodríguez-Valdez, F. Solorio-Ordaz, A. E. Chavez-Castellanos, and A. Palacio-Perez, "Homogeneous and Stratified Liquid-Liquid Flow Effect of a Viscosity Reducer: I. Comparison in parallel plates for heavy crude," *Engineering, Technology & Applied Science Research*, vol. 6, no. 6, pp. 1258–1263, Dec. 2016, https://doi.org/10.48084/etasr.876.

[3] M. Abdulkadir, D. G. Jatto, L. A. Abdulkareem, and D. Zhao, "Pressure drop, void fraction and flow pattern of vertical air–silicone oil flows using differential pressure transducer and advanced instrumentation," *Chemical Engineering Research and Design*, vol. 159, pp. 262–277, Jul. 2020, https://doi.org/10.1016/j.cherd.2020.04.009.

[4] E. J. Suarez-Dominguez, A. Palacio-Perez, J. F. Perez-Sanchez, A. Rodriguez-Valdes, S. Gonzalez-Santana, and E. Izquierdo-Kulich, "Molecular interactions between heavy crude oil and a flow enhancer in a pipeline for pressure drop reduction," *Colloids and Surfaces A: Physicochemical and Engineering Aspects*, vol. 627, Oct. 2021, Art. no. 127134, https://doi.org/10.1016/j.colsurfa.2021.127134.

[5] L. A. Abdulkareem, "Identification of Oil-Gas Two Phase Flow in a Vertical Pipe using Advanced Measurement Techniques," *Engineering, Technology & Applied Science Research*, vol. 10, no. 5, pp. 6165–6171, Oct. 2020, https://doi.org/10.48084/etasr.3679.

[6] V. A. Musa, L. A. Abdulkareem, and O. M. Ali, "Experimental Study of the Two-Phase Flow Patterns of Air-Water Mixture at Vertical Bend Inlet and Outlet," *Engineering, Technology & Applied Science Research*, vol. 9, no. 5, pp. 4649–4653, Oct. 2019, https://doi.org/10.48084/etasr.3022.

[7] J. R. Thome, "Chapter 13," in *Engineering Data Book III*, Wolverine Tube, Inc, 2004.

[8] R. C. Martinelli, "Prediction of Pressure Drop during Forced-Circulation Boiling of Water," *Transactions of the ASME*, vol. 70, pp. 695–702, 1948.

[9] D. Chisholm, "Pressure gradients due to friction during the flow of evaporating two-phase mixtures in smooth tubes and channels," *International Journal of Heat and Mass Transfer*, vol. 16, no. 2, pp. 347–358, Feb. 1973, https://doi.org/10.1016/0017-9310(73)90063-X.

[10] L. Friedel, "Improved Friction Pressure Drop Correlation for Horizontal and Vertical Two-Phase Pipe Flow," in *European Two-Phase Flow Group Meet*, Ispra, Italy, 1979.

[11] A. Lobo de Souza and M. de Mattos Pimenta, "Prediction of Pressure Drop During Horizontal Two-Phase Flow of Pure and Mixed Refrigerants," *Asme-Publications-Fed*, vol. 210, pp. 161–172, 1995.

[12] K. Mishima and T. Hibiki, "Some characteristics of air-water two-phase flow in small diameter vertical tubes," *International Journal of Multiphase Flow*, vol. 22, no. 4, pp. 703–712, Aug. 1996, https://doi.org/10.1016/0301-9322(96)00010-9.

[13] I. Y. Chen, K. S. Yang, and C.-C. Wang, "Two-Phase Pressure Drop of Air-Water in Small Horizontal Tubes," *Journal of Thermophysics and Heat Transfer*, vol. 15, no. 1–4, pp. 409–415, Oct. 2001, https://doi.org/10.2514/2.6643.

[14] A. Cavallini, G. Censi, D. Del Col, L. Doretti, G. A. Longo, and L. Rossetto, "Condensation of Halogenated Refrigerants Inside Smooth Tubes," *HVAC&R Research*, vol. 8, no. 4, pp. 429–451, Oct. 2002, https://doi.org/10.1080/10789669.2002.10391299.

[15] M. B. Ould Didi, N. Kattan, and J. R. Thome, "Prediction of two-phase pressure gradients of refrigerants in horizontal tubes," *International Journal of Refrigeration*, vol. 25, no. 7, pp. 935–947, Nov. 2002, https://doi.org/10.1016/S0140-7007(01)00099-8.

[16] G. R, "Investigation of liquid hold-up, flow resistance and heat transfer in circulation type evaporators. 4. Two-phase flow resistance in boiling refrigerants," presented at the Heat and mass transfer in refrigeration systems and in air conditioning, Freudenstadt, Germany, Sep. 1972.

[17] H. Muller-Steinhagen and K. Heck, "A simple friction pressure drop correlation for two-phase flow in pipes," *Chemical Engineering and Processing: Process Intensification*, vol. 20, no. 6, pp. 297–308, Nov. 1986, https://doi.org/10.1016/0255-2701(86)80008-3.

[18] K.-I. Choi, A. S. Pamitran, C.-Y. Oh, and J.-T. Oh, "Two-phase pressure drop of R-410A in horizontal smooth minichannels," *International Journal of Refrigeration*, vol. 31, no. 1, pp. 119–129, Jan. 2008, https://doi.org/10.1016/j.ijrefrig.2007.06.006.

[19] L. Sun and K. Mishima, "Evaluation Analysis of Prediction Methods for Two-Phase Flow Pressure Drop in Mini-Channels," in *16th International Conference on Nuclear Engineering*, Orlando, FL, USA, Dec. 2008, pp. 649–658, https://doi.org/10.1115/ICONE16-48210.

[20] J. Lee and I. Mudawar, "Two-phase flow in high-heat-flux micro-channel heat sink for refrigeration cooling applications: Part II—heat transfer characteristics," *International Journal of Heat and Mass Transfer*, vol. 48, no. 5, pp. 941–955, Feb. 2005, https://doi.org/10.1016/j.ijheatmasstransfer.2004.09.019.

[21] W. Zhang, T. Hibiki, and K. Mishima, "Correlations of two-phase frictional pressure drop and void fraction in mini-channel," *International Journal of Heat and Mass Transfer*, vol. 53, no. 1, pp. 453–465, Jan. 2010, https://doi.org/10.1016/j.ijheatmasstransfer.2009.09.011.

[22] X. Fang, Y. Xu, and Z. Zhou, "New correlations of single-phase friction factor for turbulent pipe flow and evaluation of existing single-phase friction factor correlations," *Nuclear Engineering and Design*, vol. 241, no. 3, pp. 897–902, Mar. 2011, https://doi.org/10.1016/j.nucengdes.2010.12.019.

[23] Y. Xu, X. Fang, X. Su, Z. Zhou, and W. Chen, "Evaluation of frictional pressure drop correlations for two-phase flow in pipes," *Nuclear Engineering and Design*, vol. 253, pp. 86–97, Dec. 2012, https://doi.org/10.1016/j.nucengdes.2012.08.007.

[24] A. S. Dalkilic, O. Agra, I. Teke, and S. Wongwises, "Comparison of frictional pressure drop models during annular flow condensation of R600a in a horizontal tube at low mass flux and of R134a in a vertical tube at high mass flux," *International Journal of Heat and Mass*

Transfer, vol. 53, no. 9, pp. 2052–2064, Apr. 2010, https://doi.org/10.1016/j.ijheatmasstransfer.2009.12.051.

[25] W. Li and Z. Wu, "A general correlation for adiabatic two-phase pressure drop in micro/mini-channels," *International Journal of Heat and Mass Transfer*, vol. 53, no. 13, pp. 2732–2739, Jun. 2010, https://doi.org/10.1016/j.ijheatmasstransfer.2010.02.029.

[26] D. F. Sempertegui-Tapia and G. Ribatski, "Two-phase frictional pressure drop in horizontal micro-scale channels: Experimental data analysis and prediction method development," *International Journal of Refrigeration*, vol. 79, pp. 143–163, Jul. 2017, https://doi.org/10.1016/j.ijrefrig.2017.03.024.

[27] S. Novianto, A. S. Pamitran, R. Koestoer, and K. Saito, "Two-phase Frictional Pressure Drop of Propane with Prediction Methods of Viscosity and Density in 500 μm Diameter Tube," *IOP Conference Series: Materials Science and Engineering*, vol. 316, Nov. 2018, Art. no. 012058, https://doi.org/10.1088/1757-899X/316/1/012058.

[28] O. J. Kwon, B. Shon, and Y. T. Kang, "Experimental investigation on condensation heat transfer and pressure drop of a low GWP refrigerant R-1233zd(E) in a plate heat exchanger," *International Journal of Heat and Mass Transfer*, vol. 131, pp. 1009–1021, Mar. 2019, https://doi.org/10.1016/j.ijheatmasstransfer.2018.11.114.

[29] Z. Liu, R. Liao, W. Luo, J. X. F. Ribeiro, and Y. Su, "Friction pressure drop model of gas-liquid two-phase flow in an inclined pipe with high gas and liquid velocities," *AIP Advances*, vol. 9, no. 8, Aug. 2019, Art. no. 085025, https://doi.org/10.1063/1.5093219.

[30] W. H. McAdams, "Vaporization inside horizontal tubes-II, Benzene oil mixtures," *Trans. ASME*, vol. 64, pp. 193–200, 1942.

[31] D. Chisholm, "A theoretical basis for the Lockhart-Martinelli correlation for two-phase flow," *International Journal of Heat and Mass Transfer*, vol. 10, no. 12, pp. 1767–1778, Dec. 1967, https://doi.org/10.1016/0017-9310(67)90047-6.

[32] A. J. Ghajar and C. C. Tang, "Heat Transfer Measurements, Flow Pattern Maps, and Flow Visualization for Non-Boiling Two-Phase Flow in Horizontal and Slightly Inclined Pipe," *Heat Transfer Engineering*, vol. 28, no. 6, pp. 525–540, Jun. 2007, https://doi.org/10.1080/01457630701193906.

[33] M. J. Vaze and J. Banerjee, "Experimental visualization of two-phase flow patterns and transition from stratified to slug flow," *Proceedings of the Institution of Mechanical Engineers, Part C: Journal of Mechanical Engineering Science*, vol. 225, no. 2, pp. 382–389, Feb. 2011, https://doi.org/10.1243/09544062JMES2033.

[34] O. Baker, "Design of Pipelines for the Simultaneous Flow of Oil and Gas," in *Fall Meeting of the Petroleum Branch of AIME*, Dallas, USA, Oct. 1953.

[35] R. Tahery and S. Ehterami, "Two-phase Frictional Pressure Drop in Horizontal Channels," in *7th International Chemical Engineering Congress & Exhibition*, Kish, Iran, Nov. 2011.

[36] M. Mirzania, "Investigation and modelling of pressure drop for two-phase flow in wells and inclined pipes," Tarbiat Modares University, Iran, 2005.